DOI: 10.1002/ejic.200900194

The Role of Amine–$B(C_6F_5)_3$ Adducts in the Catalytic Reduction of Imines with H_2: A Computational Study

Timofei Privalov*[a]

Keywords: Hydrogenation / Density functional calculations / Amines / Boranes / Autocatalysis

This study thoroughly examines the potential energy surfaces (PESs) of two possible mechanisms for reduction of imines by $B(C_6F_5)_3$ and H_2. The key reaction steps of the first catalytic mechanism, which is the focus of our study, are: (i) the uptake of H_2 by a thermally activated amine–$B(C_6F_5)_3$ species; (ii) proton transfer from the NH_2^+ moiety of $[RNH_2CH_2R']^+[HB(C_6F_5)_3]^-$ to the imine; (iii) nucleophillic attack of the C-center of the iminium ion by the BH^- group. The potential energy barriers of the latter, as determined by calculating the evolution of the H-bonded complex of an imine and $[RNH_2CH_2R']^+[HB(C_6F_5)_3]^-$ in toluene, are around 10 kcal mol^{-1} each. In the second mechanism, only imines serve as basic partners of $B(C_6F_5)_3$ in the H_2 activation, which affords an $[RN(H)CHR']^+[HB(C_6F_5)_3]^-$ ion pair; direct reduction then proceeds via nucleophilic attack of the C-center by the BH^- in $[RN(H)CHR']^+[HB(C_6F_5)_3]^-$. This route becomes catalytic when the product amine is released into the solvent and $B(C_6F_5)_3$ is re-used for H_2 activation. Upon taking into account the association energy of an amine–$B(C_6F_5)_3$ adduct [–9.5 kcal mol^{-1} for *t*BuN(H)CH_2Ph and $B(C_6F_5)_3$ in toluene], the potential energy barrier for H_2 uptake by an imine and $B(C_6F_5)_3$ increases to 14.5 kcal mol^{-1}. We report a somewhat lower potential energy barrier for H_2 uptake by thermally activated amine–$B(C_6F_5)_3$ adducts [12.7 kcal mol^{-1} for the B-N adduct of *t*BuN(H)CH_2Ph and $B(C_6F_5)_3$ in toluene], although the difference between the two H_2 activation barriers is within the expected error of the computational method. Two catalytic routes are compared based on B3LYP-computed PESs in solvent (toluene).

Introduction

Since Sabatier's discovery of nickel-mediated catalytic hydrogenation, which dates back to 1897, the addition of molecular hydrogen to unsaturated organic compounds has become one of the most important methods used worldwide for the production and synthesis of an extremely large variety of products and chemicals.[1] Our interest in the reduction of imines is justified by the fact that this process, as well as the reduction of nitriles, is undoubtedly one of the best synthetic methods for generating primary and secondary amines, a method that has found a great many uses in the pharmaceutical and chemical industry.[1a,2]

Typically, transition-metal-catalyzed hydrogenation reactions,[3–5] which use H_2 directly, rely on the oxidative addition of molecular hydrogen, although the heterolytic cleavage of H_2 could also afford a metal hydride in some cases,[6,7] and reductive elimination of an unsaturated acceptor at a metal center. It is noteworthy that the addition of hydrogen can also be accomplished via transition-metal-catalyzed transfer hydrogenation, where hydrogen gas is replaced by, for example, 2-propanol or formic acid;[8] asymmetric transfer hydrogenations of ketones and imines with chiral catalysts have been reported to produce enantiomerically enriched products.[9] A few different, metal-free, approaches to hydrogenation are known, for example stoichiometric reductions by main group hydrides,[10] organocatalyzed hydrogenations using the Hantzsch ester as H_2 source,[11] the reduction of alkenes by successive hydroboration/hydrogenolysis reactions,[12] and the catalytic reduction of benzophenone[13] using KO*t*Bu/H_2.

The development of metal-free catalytic processes that do not require harsh reaction conditions is motivated by the desire to replace expensive and potentially toxic precious-metal catalysts and to address the issue of chemical waste. Very recently, the Lewis base-Lewis acid cooperation in "frustrated Lewis pairs" (FLPs)[14,15] has emerged as a new concept of reactivity and catalysis.[16] The fact that steric factors can prevent the formation of a donor-acceptor[17] complex between a sterically hindered Lewis base and Lewis acid has been known for quite a while.[10,18] However, the chemical potential of such a system was not realized until the metal-free activation of H_2 by FLPs was demonstrated by Bertrand's and Stephan's groups.[19–21] The metal-free hydrogenation of imines and nitriles mediated by bulky Lewis acid-Lewis base systems,[22–27] and the $B(C_5F_5)$-catalyzed hydrosilylation of imines,[28] are just a few examples of emerging applications of FLPs which are relevant for our computational study.

[a] Department of Organic Chemistry, Arrhenius Laboratory, Stockholm University,
10691 Stockholm, Sweden
E-mail: priti@organ.su.se

Supporting information for this article is available on the WWW under http://www.eurjic.org or from the author.

There has been systematic focus on theoretical studies of the process of H_2 activation by the Lewis acid $B(C_6F_5)_3$ and a Lewis base,[29–34] and there have also been mechanistic studies regarding the catalytic reduction of imines by $B(C_6F_5)_3$-containing species.[27,35–38]

We became motivated to launch a thorough computational comparison of amine–borane mediated and autocatalytic pathways of the novel reaction in which the electron-deficient Lewis acid $B(C_6F_5)_3$ facilitates the catalytic hydrogenation of bulky imines, such as *t*BuNC(H)Ph, in the presence of H_2 at moderately elevated temperatures [Equation (1)]. Although the direct hydrogenation of bulky imines with $B(C_6F_5)_3$ and H_2, and the temperature-controlled autocatalytic pathway, have already been investigated, only a qualitative description of the related amine–borane route has been reported to the best of our knowledge.[38] The key difference between the two mechanisms in Equation (1) resides in whether the product amine–boranes become directly involved in H_2 activation or not.[35,36] There has, to date, been no accurate comparison of these two complete pathways in Equation (1). A thorough understanding of the reduction process is therefore of significant importance for the rational development and advancement of main group "frustrated Lewis pairs"-based catalysis, which is a rapidly growing area of interest.

$$\underset{\mathbf{2}}{RN{=}CR'(H)} \xrightarrow[\underset{\mathbf{1}}{B(C_6F_5)_3}]{+\,H_2} \underset{\mathbf{2'}}{RN(H)CR'(H)_2} \qquad (1)$$

Thus, the objective of our study was to compare the complete energy profiles for the different reaction routes in Equation (1) with the specific aim of gaining an insight into the following key processes: (i) initiation of the reaction and evolution of an iminium-hydridoborate ion pair; (ii) evolution of the amine–boron adducts and the interplay between imines and amines as Lewis base partners of $B(C_6F_5)_3$ in the H_2 activation step; (iii) evolution of the H-bonded complex of an ammonium-hydridoborate ion pair and an imine.

Results and Discussion

Our computational model consists of the Lewis acid $B(C_6F_5)_3$ (**1**), the imine *t*BuN=CPh(H) (**2**), and the corresponding amine **2′**. The approach which will allow us to draw reliable mechanistic conclusions and to investigate the complete energy profile of each of the pathways in Equation (1) involves mapping the potential energy surface (PES) as a function of molecular configuration using density functional electronic structure calculations. The size of the complete molecular model precludes the use of direct wavefunction-based computational methods, although DFT methods are well suited for studies of large molecular systems as they give a good compromise between accuracy and computational costs.[39]

To summarize the computational methods employed, the lowest energy conformers of all intermediates and transition states were identified at the B3LYP level of theory employing the 6-31+G* basis set (6-31++G** for all N- and B-bound hydrogen atoms, as well as for H_2). While all figures presented herein show the B3LYP-based structures, all key reaction steps were validated against the MPW1K and BHandHLYP data. All reported barriers are consistent across the three functionals. The B3LYP functional was also validated against the MP2 data for enthalpy change for reduction of imines at the 6-311++G** basis set level (see Supporting Information). All reported potential energies were re-computed with the 6-31++G** basis set in toluene for the lowest energy conformers of all intermediates (stationary points of PESs) and transition states. All transition states were validated by additional QST-guided calculations. The connectivity between transition states and appropriate intermediates was confirmed by intrinsic reaction coordinate (IRC) scans, and solvent effects were accounted for within the self-consistent polarizable continuum model (SCRF/PCM). Further details of the computational procedures can be found in the Computational Details section; validation studies are reported in the Supporting Information.

Direct Autocatalytic Reduction of Imine by $B(C_6F_5)_3$ and H_2

A plausible route, which has been proposed by Stephan's group and rationalized theoretically by Papai's group,[36,38] describes the reduction of imines by $B(C_6F_5)_3$ and H_2, as follows: (i) heterolytic H_2 splitting by an imine and $B(C_6F_5)_3$, and (ii) nucleophilic attack of the iminium carbon by the borohydride moiety. As a result, formation of a B–N-bonded adduct between the product amine and $B(C_6F_5)_3$ is anticipated. In order to be able to draw a quantitative comparison at the same level of theory with the direct route with the more complex catalytic pathway involving amine–borane adducts (see below), we performed straightforward B3LYP-based calculations of the former.

The B3LYP-computed transition state of the heterolytic splitting of H_2 by a model imine [*t*BuNC(H)Ph] and $B(C_6F_5)_3$ is shown in Figure 1. The transition state **TS1** represents the true saddle-point[40] and is similar to previously reported results of Papai et al.[38,41] As expected,[27,29,38] the solvent-corrected potential energy barrier of H_2 splitting is remarkably low: B3LYP functional calculations predict that **TS1** is only 5.0 kcal mol^{-1} higher than the total energy of reacting species, namely *t*BuNC(H)Ph, $B(C_6F_5)_3$, and H_2. The thermochemical correction to the potential energy barrier of H_2 uptake is about 11 kcal mol^{-1}.

The splitting of H_2 by the imine-borane Lewis pair is exothermic and affords iminium-hydridoborate ionic complex **3** (Figure 2). The B3LYP-computed proton-hydride hydrogen bond,[42,43] a $BH^{-}\cdots{}^{+}HN$ close contact, and the linear alignment of the BH^- and NH^+ moieties in **3** are in agreement with previously reported theoretical and experimental data for $BH^{-}\cdots{}^{+}HP$ and $BH^{-}\cdots{}^{+}HN$ contacts.[27,29,36]

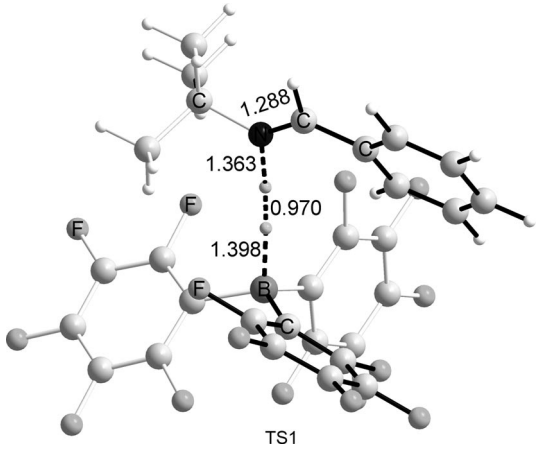

Figure 1. The transition state for the heterolytic splitting of H_2 by the imine-borane pair. Dashed lines highlight B–H, H–H, and N–H distances; all H···F close contacts have been omitted for simplicity. All distances given in Å.

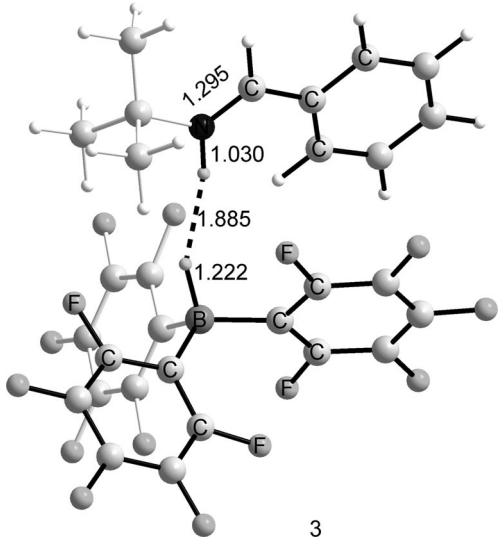

Figure 2. The optimized hydridoborate complex with the iminium ion. Dashed lines highlight H^+–H^- distances; all H···F close contacts have been omitted for simplicity. All distances are given in Å.

The nucleophilic attack on the carbon atom of the iminium ion in **3** by the BH^- unit of the borohydride is described by the true transition state **TS2** (Figure 3), which has a B3LYP-computed potential energy barrier of 12.4 kcal mol^{-1}. Transition state **TS2** represents the true saddle-point on the direct route from **3** to the amine–borane couple, which collapses to afford **4** (see Supporting Information) in a straightforward fashion.

The B3LYP-based relative potential energies for the reduction of *t*BuN=CPh(H) by $B(C_6F_5)_3$ and H_2, and the corresponding catalytic mechanism, are summarized in Scheme 1. The direct reduction pathway is characterized by relatively low barriers and all steps leading to B–N adduct **4** are exothermic. Overall, our results are in a good agreement with previously published PES calculations.[38]

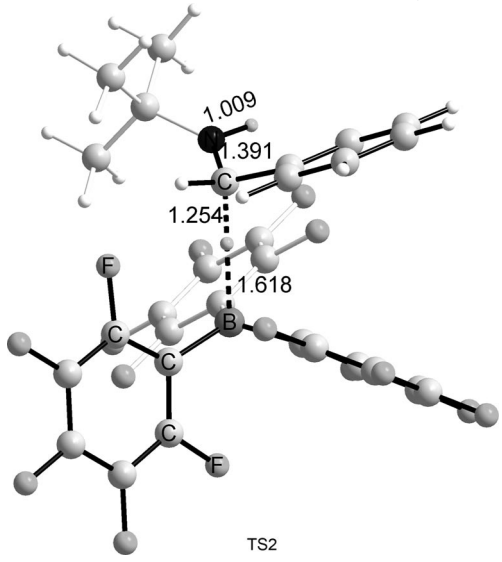

Figure 3. **TS2**: The transition state of the nucleophilic attack of the iminium carbon; dashed lines highlight B–H and H–N distances; all H···F close contacts have been omitted for simplicity. All distances are given in Å.

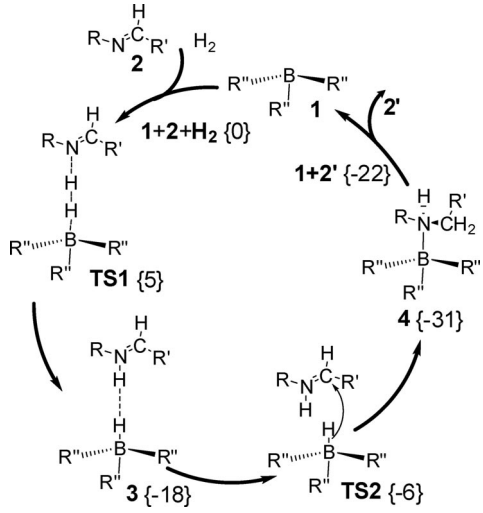

Scheme 1. Auto-catalyzed reduction of imines by $B(C_6F_5)_3$ (**1**) and H_2 occurs as follows: **1** + **2** + H_2 → **TS1** → **3** → **TS2** → **4** → **TS3** → **1** + **2′**. The relative potential energies, computed at the B3LYP/6-31++G** level in toluene (PCM model) for *t*BuN=CPh(H), are reported in brackets. All energies are given in kcal mol^{-1}.

Ammonium-Hydridoborate Ion Pair and Reduction of Imines with H_2

According to Scheme 1, the reduction of *t*BuN=CPh(H) by $B(C_6F_5)_3$ and H_2 proceeds in an autocatalytic fashion if amine–borane complex **4** dissociates, which implies that the potential energy barrier of H_2 uptake by the re-used $B(C_6F_5)_3$ and an imine increases in energy by an amount approximately equal to the association energy (E_{ae}) in **4**.[44] Thus, after the first turnover of the autocatalytic reduction, the effective potential energy barrier of H_2 activation be-

comes at least 14.5 kcal mol^{-1}. Thermal activation is therefore likely to be necessary to promote dissociation of the B–N-bonded adduct **4**.[36,38]

The association energy of **4** depends strongly on the steric encumbrance of the amine. Indeed, the B–N-bonded amine–borane adduct $CH_3(PhCH_2)N(H)\cdot B(C_6F_5)_3$ (**4′**) is predicted to have quite a large association energy of around –20 kcal mol^{-1} and a potential energy barrier of dissociation of around 23 kcal mol^{-1} (toluene solvent). The computed amine–borane association energy seems to be somewhat smaller for bulky amines [–9.5 and –10.3 kcal mol^{-1} for tBu$(PhCH_2)N(H)\cdot B(C_6F_5)_3$, as calculated with the density functionals B3LYP and MPW1K (toluene solvent)].[45] This implies that the association energy of the amine–$B(C_6F_5)_3$ adduct becomes a major contributor to the rate-limiting step after the first catalytic turnover and that, depending on the steric hindrance of the amine, $B(C_6F_5)_3$ might not become re-usable even at elevated temperatures. If the amine–boron adducts are too stable to dissociate, re-use of the Lewis acid $B(C_6F_5)_3$ is blocked and the reduction appears to be stoichiometric.

An alternative to the autocatalytic reduction of an imine by $B(C_6F_5)_3$ and H_2 is a process which is initiated by the reaction of an amine–borane couple with H_2. The resulting ammonium ion-hyridoborate complex **3′** has been identified by NMR spectroscopy and X-ray crystallography;[36] H_2 activation by an amine–$B(C_6F_5)_3$ adduct has been rationalized previously[38] and is briefly addressed herein.

First, similarly to the ionic complex **3**, the optimized geometry of the hydridoborate adduct with the ammonium ion (**3′**; Figure 4) reveals $H^+\cdots H^-$ bonding. The B3LYP-computed H–H distance of 1.588 Å is somewhat longer in **3′** than the crystallographic value of 1.87(3) Å. However, the computed H–H distance and its deviation from the crystallographic data (approx. 0.3 Å) are both in agreement with computational results obtained for a similar FLP compound.[27] Our results are also in good agreement with fully optimized structures at the M05-2X DFT level.[38] The consistent discrepancy between the computed and crystallographic H–H distances for known FLP complexes could be explained, as pointed out previously,[27] by the tendency of the X-ray technique to yield too short X–H bonds.[46]

Secondly, the splitting of H_2 by the amine–boron couple is predicted to be more exothermic than in the direct pathway $-\Delta E$ is –23.4 kcal mol^{-1} relative to **1** + **2′** + H_2 (–13.9 kcal mol^{-1} with respect to **4** + H_2), whereas the corresponding potential energy barrier is predicted to be only 3.2 kcal mol^{-1} (B3LYP), which is somewhat smaller than that for H_2 uptake by an imine and $B(C_6F_5)_3$. The difference between the two is nevertheless within the error of the computational method.

Transition states **TS1′** and **TS1** have similar key geometrical features, namely a significant elongation of the H–H bond and an elongation of the N–C bond of the proton acceptor with respect to the isolated imine/amine, respectively.[47] The basicity of the N atom is important for the splitting of H_2: an amine is a better base and this is why, we believe, the splitting of H_2 by the amine–borane couple

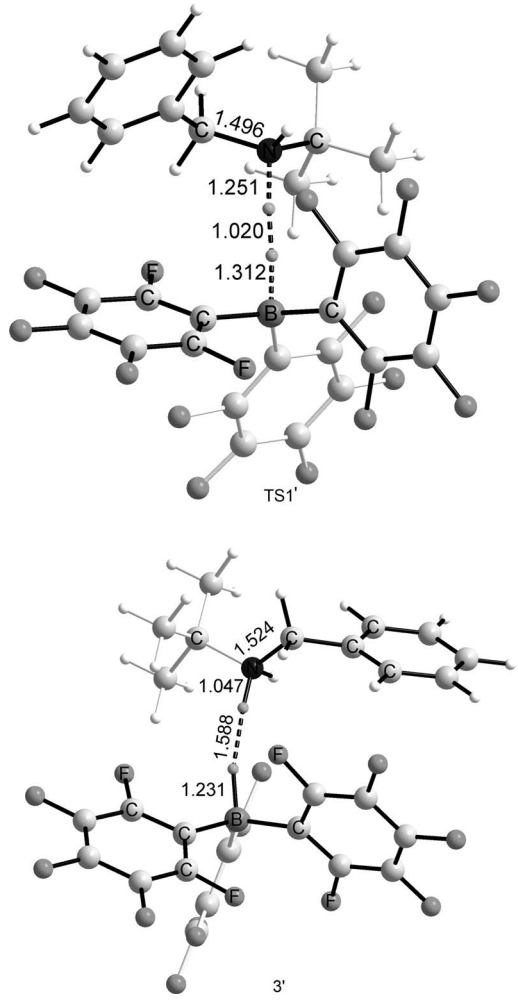

Figure 4. **TS1′**: The transition states for the heterolytic splitting of H_2 by the amine–borane couple. Dashed lines highlight B–H, H–H, and N–H distances. **3′**: The hydridoborate adduct with the ammonium ion. The dashed lines highlight H^+–H^- distances. All H···F close contacts have been omitted for simplicity. All distances are given in Å.

is more exothermic (see Scheme 1). The potential energy barrier for **1** + **2′** + H_2 → **3′** is lower than **TS1**. However, as illustrated in Figure 5, the association energy of **4** increases the potential energy barrier for H_2 splitting by the B–N-bonded amine–borane adduct (**4** + H_2 → **3′**), in agreement with recent experimental and computational data.[36,38]

While the iminium-hydridoborate pair **3** seems to have only one evolutionary pathway available, namely nucleophilic attack by the BH^- group, the presence of the ammonium ion in **3′** suggests a new reaction route in the presence of imines. Indeed, H-bonding between the N atom of the imine and one of the NH_2 protons is most likely to afford complex **5** (Figure 6). The evolution of such a complex is the key to understanding the complete catalytic mechanism of the reaction in Equation (1). Proton exchange between an ammonium ion and an imine has been observed experimentally for a number of related species.[8a] Furthermore, the catalytic reduction of an unsaturated C=X bond, where

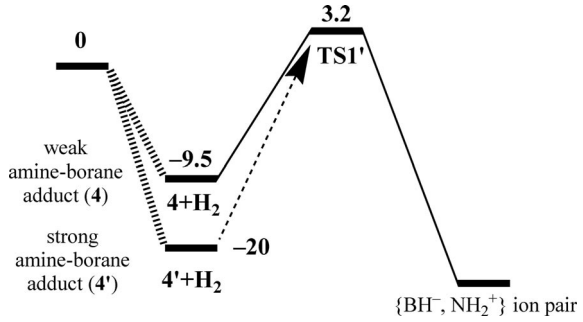

Figure 5. Qualitative relationship between the potential energy barrier for splitting of H_2 (**4** + H_2 → **3′**) and the association energy of the amine–borane adduct **4** in toluene. All data were computed at the B3LYP/6-31++G** level in toluene (PCM model) with respect to the dissociation limit (free reacting species). **4′** is the strong amine–borane adduct $CH_3(PhCH_2)N(H)\cdot B(C_6F_5)_3$. MPW1K, BH, and HLYP potential energy barriers deviate from the B3LYP data by less than 1.5 kcal mol^{-1}. All energies are given in kcal mol^{-1}.

X is a heteroatom, is typically initiated by the protonation step.[8a] A simplified model in which an imine is H-bonded to an ammonium ion, [*t*BuNCPh(H)·*t*BuN(H)$_2$CH$_2$Ph]$^+$ (**6**), can be used to estimate the energy change and the potential energy barrier for proton transfer from the NH_2 moiety to the imine. The proton transfer in **6** is endothermic by 2.8 kcal mol^{-1}, while the potential energy barrier for the proton transfer in **6** is only 7.4 kcal mol^{-1} in toluene. It is therefore quite plausible that proton transfer to the imine affords the hydridoborate complex with the iminium ion and the H-bonded amine (complex **5′** in Figure 6).

Validation of the two-step mechanism involving proton and hydride transfers proposed herein is based on thorough PES scans (see below). Although the transformation **5** → **5′** is endothermic by 3.2 kcal mol^{-1} in toluene, the corresponding potential energy barrier is only 10.4 kcal mol^{-1}. This agrees well with the results obtained in a much simpler model (**6**). The transition state of the proton transfer in **5** (**TS3** in Figure 7) is the true saddle-point that connects true stationary intermediates **5** and **5′**. It is noteworthy that the proton donor and the proton acceptor are positioned closer to the hydridoborate in the transition state structure than in intermediates **5** and **5′**, and that the H_B–C distance in intermediate **5′** is shorter than that in **5**.

We were also able to locate the true transition state of the nucleophilic attack of the iminium carbon (**TS2′** in Figure 8), which is similar to**TS2** as regards its key geometrical features, although the B–C distance is around 0.2 Å longer in the former. The amine stays further away from the boron atom in **TS2′** than in intermediates **5** and **5′**. With respect to intermediate **5**, the potential energy barrier is 12.8 kcal mol^{-1} for **TS2′** in toluene. An intrinsic reaction coordinate scan revealed that the crossing of **TS2′** leads to collapse of the amine–borane complex towards the final B–N-bonded adduct with the outer-sphere bound amine.

The potential energy profile for reduction of the model imine *t*BuN=CPh(H) by the B–N-bonded adduct between *t*BuNHCPh(H)$_2$, B(C$_6$F$_5$)$_3$, and H_2 by is summarized in Figure 9 according to the proposed catalytic mechanism in

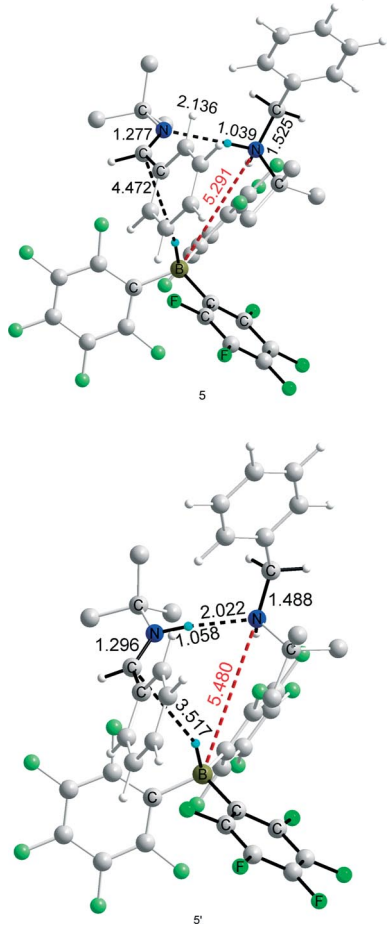

Figure 6. **5**: The hydridoborate adduct with the ammonium ion and the H-bonded imine. **5′**: The hydridoborate complex with the iminium ion and the amine. Hydrogen atoms of *t*Bu groups and all H···F close contacts have been omitted for simplicity. Red dashed lines highlight the B–N distances, the black dashed lines highlight the H_B–C and N–H distances. All distances are given in Å.

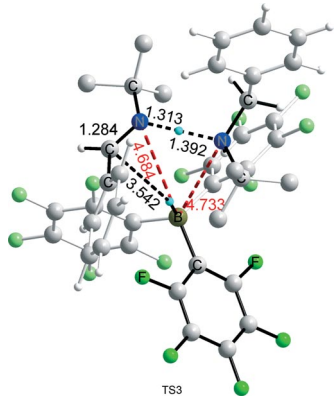

Figure 7. The transition state for proton transfer from the ammonium ion to the imine in the presence of the hydridoborate. Hydrogen atoms of *t*Bu groups and all H···F close contacts have been omitted for simplicity. Red dashed lines highlight the B–N distances, the black dashed lines highlight the H_B–C and N–H distances. All distances are given in Å.

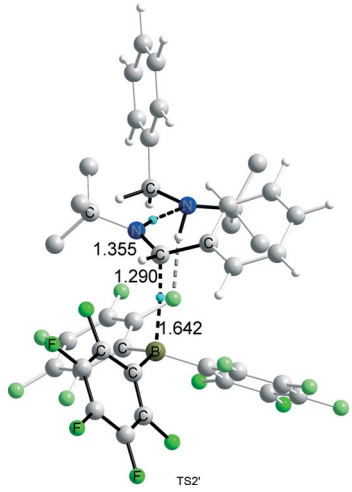

Figure 8. The transition state for the nucleophilic attack of the C-centre in **5′**. Hydrogen atoms of *t*Bu groups and all H···F close contacts have been omitted for simplicity. B–N distances are 3.660 and 5.587 Å for the N(imine) and N(amine), respectively. Black dashed lines highlight the N–H, B–H and C–H distances. All distances are given in Å.

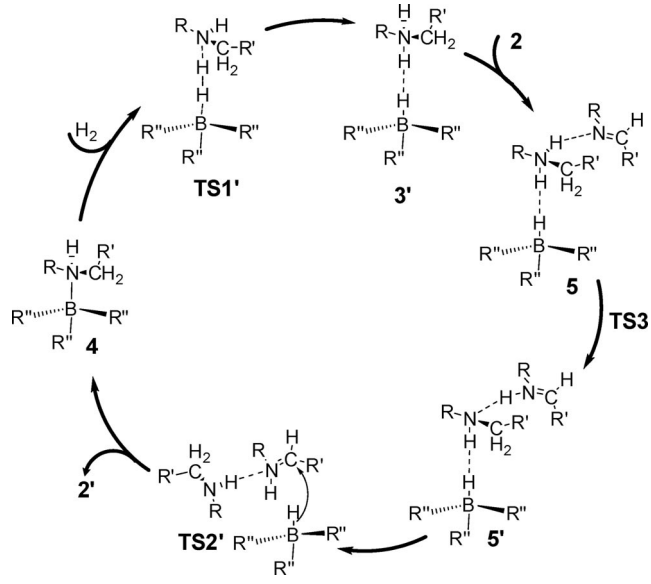

Scheme 2. Catalytic reduction of imines by **1** and H_2 via: (i) H_2 activation by an amine–borane complex (**4** + H_2 → **3′**), (ii) hydrogen bonding of an imine and **3′** (**3′** + **2** → **5**), and (iii) subsequent two-step reduction of an amine in **5**.

Scheme 2. It is noteworthy that the transition state for the activation of molecular hydrogen by **4** should increase by around 11 kcal mol^{-1} due to the thermochemical corrections (the *–ST* term in the Gibbs free energy definition is the major contributor), while **TS3** and **TS2′** should be affected to a much lesser degree. The binding of an imine (**3′** + **2** → **5**) is slightly endothermic (by 3.2 kcal mol^{-1}) in the gas phase and slightly exothermic (by –1.3 kcal mol^{-1}) in toluene. In the gas phase, the stabilizing effect of the H-bonding between the proton acceptor and the proton donor does not outweigh the increase of the potential energy due to the increased separation between the hydridoborate and the NH_2^+ moiety. This explains the gas phase result, while solvent effects in toluene tend to stabilize the hydridoborate-NH_2^+ complex **5** more than complex **3′**.

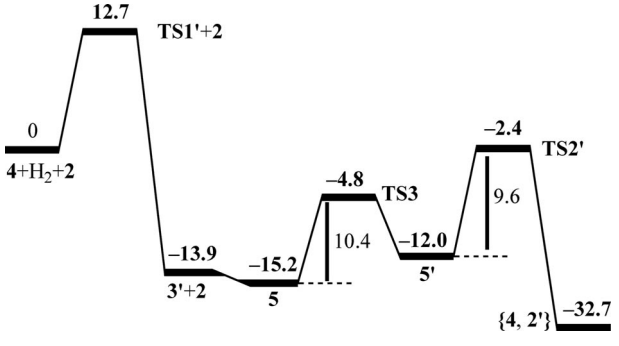

Figure 9. Summary of the PES for the reduction of *t*BuN=CPh(H) by **4** and H_2 in toluene for the two-step pathway starting from the reacting species. H_2 activation appears to be the rate-limiting step. All energies are given in kcal mol^{-1}.

According to our calculations, the $[RNH_2CH_2R']^+[HB(C_6F_5)_3]^-$ ion pair appears to be an efficient and flexible source of the proton and the hydride for the reduction of moieties containing unsaturated N=C bonds. A comparison of the potential energies of the direct autocatalytic pathways (Scheme 1) with the PES in Figure 9 reveals that the potential energy barriers of the nucleophilic attack, computed at the same level of theory, are similar in both pathways. Proton transfer from the NH_2^+ group to an imine is also allowed due to a relatively low barrier. The activation of molecular hydrogen by the amine–borane adduct **4** is the rate-limiting step for a bulky imine [*t*BuN=CPh(H) in our mode], and this becomes clearer for a less bulky one, as illustrated in Figure 5 for MeN=CPh(H). Furthermore, the difference between the barriers of H_2 activation in both catalytic pathways is within the error of the computational methods, which means that both mechanisms (Schemes 1 and 2) could operate with similar efficiency (see the combined mechanistic proposal given in the Supporting Information).

A straightforward potential energy scan of the H^- transfer to the C-center without prior protonation of the N center of the imine convinced us that such a process is unlikely and that protonation of the imine is the key step.[38] This agrees with experimental results from Stephan's studies. Since complex **5** has the characteristic features of the bifunctional Shvo catalyst, for which a concerted pathway for imine reduction has been proposed,[48] we investigated the likelihood of such a pathway. We attempted to locate the concerted transition state which should correspond hypothetically to the synchronized protonation of the imine and the nucleophilic attack of the C center of the imine in complex **5**. No such transition was found, which is not surprising considering that the C–H_B and N–H distances are quite large in the starting geometry (4.47 and 2.14 Å, respectively). It is therefore somewhat doubtful that a concerted transition state is likely to occur in our case. What we have learned from our attempts to find a concerted transition

state for the imine reduction in **5**, however, is that **TS3**, intermediate **5′**, and **TS2′** reside on the optimal (lowest potential energy) reaction pathway, which connects the starting complex **5** and the final amine–borane adduct {**4**, **2**} in a continuous fashion.

Conclusions

The present study has independently identified complete potential energy surfaces (PESs) for two possible routes for the reduction of imines by $B(C_6F_5)_3$ and H_2; all calculations have been performed at the DFT level within an implicit solvent model (PCM) for the model imine *t*BuNCHPh in toluene The key difference between the two mechanisms is the Lewis basic partner of the Lewis acid $B(C_6F_5)_3$ for the heterolytic splitting of molecular hydrogen: the so-called autocatalytic mechanism involves imines as Lewis bases, while an alternative mechanism operates via amine–$B(C_6F_5)_3$ adducts. The common feature of both mechanisms is that they require elevated temperatures for sustainable operation. Our results are in agreement with the recently published computational study by Papai's group, which is primarily concerned with the autocatalytic pathway.

Since initially only imines are present in solution, the reaction is initiated by proton and hydride transfer to form an amine via an elegant two-step pathway: (i) H_2 activation by an imine-borane "frustrated Lewis pair" (FLP) affords an iminium–hydridoborate ion pair with a direct potential energy barrier of only 5 kcal mol^{-1}; (ii) nucleophilic attack of the C-center by the BH^- group transforms the $[RN(H)CHR']^+[HB(C_6F_5)_3]^-$ ion pair into an amine–$B(C_6F_5)_3$ adduct with a potential energy barrier of 12 kcal mol^{-1}. The association energy of the amine–$B(C_6F_5)_3$ adduct appears to be an obstacle for re-use of the Lewis acid. Judging by the potential energy profile, elevated temperatures are likely to be required for the liberation of $B(C_6F_5)_3$, which could than be re-used in a catalytic fashion. Thus, in light of the association energy of the amine–borane adduct [approx. –10 kcal mol^{-1} for *t*BuN(H)CH_2Ph and $B(C_6F_5)_3$ in toluene], the potential energy barrier for H_2 uptake by the model imine and the re-used $B(C_6F_5)_3$ increases to around 15 kcal mol^{-1}. Our data indicate that sterically unhindered imines might not be able to sustain the autocatalytic reduction due to the prohibitively large association energy of the corresponding amine–$B(C_6F_5)_3$ adducts.

Although elevated temperatures allow the autocatalytic reduction of sterically hindered imines to operate, we have found that a lower energy pathway of H_2 uptake becomes available as soon as the concentration of the product amines reaches a certain level. Thus, we have obtained a lower potential energy barrier for H_2 uptake by the thermally activated amine–$B(C_6F_5)_3$ adduct itself [approx. 13 kcal mol^{-1} for an adduct of *t*BuN(H)CH_2Ph and $B(C_6F_5)_3$ in toluene]. Although the energy difference between the two H_2 uptake pathways is not very large, analysis of the computed potential energy profiles unambiguously indicates that the ammonium-hydridoborate ion pair $[RNH_2CH_2R']^+[HB(C_6F_5)_3]^-$ should play a key role in the transfer of the proton and hydride to the imine, in agreement with available experimental data.

We have also computed the evolution of the H-bonded complex of an imine and $[RNH_2CH_2R']^+[HB(C_6F_5)_3]^-$. Despite apparent similarity with Shvo's catalyst, the concerted proton and hydride transfer is blocked by significant steric congestion of the hydride and proton donor moieties, as well as the proton acceptor. A direct transition state search and exploration of the potential energy surfaces has identified the true transition states responsible for the two-step reduction of an imine by $[RNH_2CH_2R']^+[HB(C_6F_5)_3]^-$. The computed potential energy barriers for the proton and hydride transfer are quite low, thereby indicating that H_2 uptake by amine–$B(C_6F_5)_3$ is the slow reaction step. Considering that the association energy of amine–$B(C_6F_5)_3$ depends on the steric hindrance of the amine, it is expected that dissociation of the B–N bond itself could become the rate-limiting step instead.

Computational Details

All calculations were performed with the Jaguar 6.0[49] quantum chemistry package. Our approach is somewhat similar to a procedure described previously.[33] Thus, we initially performed a conformational search using potential energy scans with the B3LYP functional using the split-valence double-zeta basis set, 6-31+G*,[50,51] augmented with diffuse and polarization functions, and the molecular model system formally in the gas phase. The geometries of up to ten low-energy conformers were then re-optimized using the B3LYP and MPW1K/BHandHLYP functionals[52,53] with the 6-31+G* basis set (6-31++G** for active hydrogens); all degrees of freedom were optimized. All transition states were found with B3LYP/6-31+G* (6-31++G** for active hydrogens) using the quadratic synchronous transit (QST) method, as implemented in Jaguar 6.0, and were characterized by one single imaginary vibrational frequency along the proper reaction coordinate. Intrinsic reaction coordinate scans were performed to verify that all reported transition states did indeed "connect" the appropriate intermediates along the reaction coordinate, which is defined by the Hessian at the corresponding transition state structure.

In order to increase the computational accuracy of the relative energies for all intermediates and transition states, the larger basis set 6-31++G** was used to obtain the final electronic energies of all complexes, employing geometries obtained with the 6-31+G* base set.

Solvent effects were accounted for as follows. Gas-phase optimized structures [B3LYP with the 6-31+G* basis set (6-31++G** for active hydrogens bound to N, B, and in H_2)] were used as starting structures in order to obtain energies of all intermediates and transition states in solvent within the self-consistent reaction field model[54] with toluene as solvent (ρ = 0.8669 g/mL, MW = 92.14 g mol^{-1}, dielectric constant = 2.4) at the large basis set level (6-31++G**). These data were used to construct potential energy profiles and for the discussion of relative energies in the text. To check the stability of solvated complexes, all geometries were relaxed and optimized within the self-consistent implicit solvent model (PCM).

Supporting Information (see also the footnote on the first page of this article): Coordinates and structural parameters of all optimized complexes are provided.

Acknowledgments

We thank the Swedish Research Council and the K & A Wallenberg Foundation for financial support of this work.

[1] a) J. G. de Vries, C. J. Elsevier, *The Handbook of Homogeneous Hydrogenation*, Wiley-VCH, Weinheim, **2007**; b) *Comprehensive Asymmetric Catalysis* (Eds.: E. N. Jacobsen, A. Pfaltz, H. Yamamoto), Springer, Berlin, **2004**; c) G. W. Parshall, S. D. Ittel, *Homogeneous Catalysis: The Applications and Chemistry of Catalysis by Soluble Transition Metal Complexes*, 2nd Edition, Wiley, **1992**.

[2] a) M. L. Clarke, G. J. Roff, in *The Handbook of Homogeneous Hydrogenation* (Eds.: J. G. de Vries, C. J. Elsevier), Wiley-VCH, Weinheim, **2007**, p. 413; b) W. Tang, X. Zhang, *Chem. Rev.* **2003**, *103*, 3029; c) S. Kobayashi, H. Ishitani, *Chem. Rev.* **1999**, *99*, 1069.

[3] a) G. Zassinovich, G. Mestroni, *Chem. Rev.* **1992**, *92*, 1051; b) C. F. de Graauw, J. A. Peters, H. van Bekkum, J. Huskens, *Synthesis* **1994**, 1007; c) see also J. M. Brunel, *Tetrahedron* **2007**, *63*, 3899 and references cited therein. d) For the metal-catalyzed and organocatalytic reductions of compounds containing C=N bonds, see M. Wills, *Imino Reduction by Transfer Hydrogenations*, in: *Modern Reduction Methods* (Eds.: P G. Andersson, I. J. Munslow), Wiley, **2008**, p. 271–296 and also e) H. Adolfsson, *Alkene and Imino Reductions by Organocatalysis* in *Modern Reduction Methods* (Eds.: P. G. Andersson, I. J. Munslow), Wiley, **2008**, p. 341–362.

[4] a) M. K. Whittlesey, *Comprehensive Coordination Chemistry II* (Eds.: J. McCleverty, T. Meyer), Elsevier, **2004**, vol. 9, p. 265–304; b) T. V. RajanBabu, A. L. Casalnuovo, T. A. Ayers, N. Nomura, J. Jin, H. Park, M. Nandi, *Curr. Org. Chem.* **2003**, *7*, 301.

[5] S. J. Lippard, J. M. Berg, *Principles of Bioinorganic Chemistry*, University Science Books, **1994**.

[6] M. Yamakawa, H. I. R. Noyori, *J. Am. Chem. Soc.* **2000**, *122*, 1466.

[7] K. Abdur-Rashid, A. J. Lough, R. H. Morris, *Organometallics* **2000**, *19*, 2655.

[8] a) J. S. M. Samec, J.-E. Bäckvall, P. G. Andersson, P. Brandt, *Chem. Soc. Rev.* **2006**, *35*, 237; b) G. Serafino, E. Alberico, *Chem. Soc. Rev.* **2006**, *35*, 226.

[9] a) T. Ohkuma, R. Noyori, in: *Comprehensive Asymmetric Catalysis*, vol. 1, (Eds.: E. N. Jacobsen, A. Pfaltz, H. Yamamoto), Springer, Berlin, **1999**, 199; b) S. Gladiali, E. Alberico, in *Transition Metals for Organic Synthesis*, vol. 2 (Eds.: M. Beller, C. Bolm), Wiley-VCH, Weinheim, **2004**, p. 145; c) C. Bianchini, L. Glendenning, *Chemtracts* **1997**, *10*, 333; d) H.-U. Blaser, C. Malan, B. Pugin, F. Spindler, H. Steiner, M. Studer, *Adv. Synth. Catal.* **2003**, *345*, 103; e) K. Everaere, A. Mortreux, J.-F. Carpentier, *Adv. Synth. Catal.* **2003**, *345*, 67; f) R. Noyori, S. Hashiguchi, *Acc. Chem. Res.* **1997**, *30*, 97–102; g) M. J. Palmer, M. Wills, *Tetrahedron: Asymmetry* **1999**, *10*, 2045; h) X. Wu, J. Xiao, *Chem. Commun.* **2007**, *24*, 2449.

[10] M. B. Smith, J. March, in: *March's Advanced Organic Chemistry*, New York, 5th ed., **2001**, p. 1197–1204 and p. 1544–1564.

[11] a) H. Adolfsson, *Angew. Chem. Int. Ed.* **2005**, *44*, 3340; b) P. I. Dalko, L. Moisan, *Angew. Chem. Int. Ed.* **2004**, *43*, 5138; c) M. Rueping, A. P. Antonchick, T. Theissmann, *Angew. Chem. Int. Ed.* **2006**, *128*, 12662.

[12] a) E. J. deWitt, F. L. Ramp, L. E. Trapasso, *J. Am. Chem. Soc.* **1961**, *83*, 4672; b) F. L. Ramp, E. J. deWitt, J. Trapasso, *J. Org. Chem.* **1962**, *27*, 4368; c) R. Koester, G. Bruno, P. Binger, *Justus Liebigs Ann. Chem.* **1961**, *644*, 1; d) M. W. Haenel, J. Narangerel, U. B. Richter, A. Rufinska, *Angew. Chem. Int. Ed.* **2006**, *45*, 1061.

[13] A. Berkessel, T. J. S. Schubert, T. N. Mueller, *J. Am. Chem. Soc.* **2002**, *124*, 8693.

[14] L. Cabrera, G. C. Welch, J. D. Masuda, P. Wei, D. W. Stephan, *Inorg. Chim. Acta* **2006**, *359*, 3066.

[15] G. C. Welch, J. D. Masuda, D. W. Stephan, *Inorg. Chem.* **2006**, *5*, 478.

[16] D. W. Stephan, *Org. Biomol. Chem.* **2008**, *6*, 1535.

[17] G. N. Lewis, *Valence and the Structure of Atoms and Molecules*, Chemical Catalogue Company, Inc., New York, **1923**.

[18] H. C. Brown, H. I. Schlesinger, S. Z. Cardon, *J. Am. Chem. Soc.* **1942**, *64*, 325.

[19] G. C. Welch, R. R. San Juan, F. D. Masuda, D. W. Stephan, *Science* **2007**, *314*, 1124.

[20] G. D. Frey, V. Lavallo, B. Donnadieu, W. W. Schoeller, G. Bertrand, *Science* **2007**, *316*, 439.

[21] A. L. Kenward, W. E. Piers, *Angew. Chem. Int. Ed.* **2008**, *47*, 38.

[22] P. A. Chase, G. C. Welch, T. Jurca, D. W. Stephan, *Angew. Chem. Int. Ed.* **2007**, *46*, 8050.

[23] J. S. J. McCahill, G. C. Welch, D. W. Stephan, *Angew. Chem. Int. Ed.* **2007**, *46*, 4968.

[24] G. C. Welch, L. Cabrera, P. A. Chase, E. Hollink, J. D. Masuda, P. Wei, D. W. Stephan, *Dalton Trans.* **2007**, 3407.

[25] P. Spies, G. Erker, G. Kehr, K. Bergander, R. Fröhlich, S. Grimme, D. W. Stephan, *Chem. Commun.* **2007**, 5072.

[26] G. C. Welch, D. W. Stephan, *J. Am. Chem. Soc.* **2007**, *129*, 1880.

[27] V. Sumerin, F. Schulz, M. Atsumi, M. Wang, C. Wang, M. Nieger, M. Leskela, T. Repo, P. Pyykko, B. Rieger, *J. Am. Chem. Soc.* **2008**, *130*, 14117.

[28] J. M. Blackwell, E. R. Sonmor, T. Scoccitti, W. E. Piers, *Org. Lett.* **2000**, *2*, 3921.

[29] T. A. Rokob, A. Hamza, A. Stirling, T. Soos, I. Papai, *Angew. Chem. Int. Ed.* **2008**, *47*, 2435.

[30] Y. Guo, S. Li, *Eur. J. Inorg. Chem.* **2008**, 2501.

[31] S. Li, Y. Guo, *Inorg. Chem.* **2008**, *47*, 6212.

[32] A. Stirling, A. Hamza, T. A. Rokob, I. Papai, *Chem. Commun.* **2008**, 3148.

[33] A. Staubitz, M. Besora, J. N. Harvey, I. Manners, *Inorg. Chem.* **2008**, *47*, 5910.

[34] a) V. S. Nguyen, M. H. Matus, D. J. Grant, M. T. Nguyen, D. A. Dixon, *J. Phys. Chem. A* **2007**, *111*, 8844; b) G. Gopakumar, V. S. Nguyen, M. T. Nguyen, *THEOCHEM* **2007**, *811*, 77.

[35] D. Chen, J. Klankermayer, *Chem. Commun.* **2008**, 2130.

[36] P. A. Chase, T. Jurca, D. W. Stephan, *Chem. Commun.* **2008**, 1701.

[37] T. I. Privalov, *Dalton Trans.* **2009**, 1321.

[38] T. A. Rokob, A. Hamza, A. Stirling, I. Papai, *J. Am. Chem. Soc.* **2009**, *131*, 2029.

[39] L. Noodleman, T. Lovell, W.-G. Han, J. Li, F. Himo, *Chem. Rev.* **2004**, *104*, 459.

[40] The exploration of the potential surface along the intrinsic reaction coordinate, as defined by the Hessian of the transition state, confirmed that **TS1** describes the direct route (**1** + **2** + $H_2 \rightarrow$ **3**) from reacting species to the corresponding ionic intermediate **3** (Figure 2).

[41] Some geometrical differences between the transition states reported in our study and previously published results by Papai's group are obviously due to the difference in computational methods. However, all key relative potential energy barriers reported herein are in agreement with the results in ref. 38, in which the autocatalytic route has been explored computationally.

[42] R. Custelcean, J. E. Jackson, *Chem. Rev.* **2001**, *101*, 1963.

[43] S. J. Grabowski, W. A. Sokalski, J. Leszczynski, *J. Chem. Phys.* **2007**, *337*, 68–76.

[44] This approximation is valid as long as the potential energy barrier for B–N dissociation is lower than $\Delta E^{\#}$(**TS1**) + $|E_{ae}|$. Effects such as H-bonding and cage effects in solvent could influence the actual barrier as well.
[45] The association energy of amine–borane adducts seems to be sensitive to the flexibility of the basis set. As expected, calculations with the basis set that lacks diffuse and polarization functions, i.e. a simple 6-31G basis set, predict much larger association energies even for bulky amines because of the poor description of steric congestion.
[46] G. R. Desiraju, T. Steiner, *The Weak Hydrogen Bond in Structural Chemistry and Biology*, Oxford University Press, Chichester, U.K., **1999**, p. 283–287.
[47] See also Figure S1 in the Supporting Information.
[48] C. P. Casey, G. A. Bikzhanova, Q. Cui, I. A. Guzei, *J. Am. Chem. Soc.* **2005**, *127*, 14062.
[49] Jaguar 6.0, Schrödinger, LLC, Portland, Oregon, **2005**.
[50] P. J. Hay, W. R. Wadt, *J. Chem. Phys.* **1985**, *82*, 299.
[51] a) W. J. Hehre, R. Ditchfield, J. A. Pople, *J. Chem. Phys.* **1972**, *56*, 2257; b) M. M. Francl, W. J. Pietro, W. J. Hehre, J. S. Binkley, M. S. Gordon, D. J. Defrees, J. A. Pople, *J. Chem. Phys.* **1982**, *77*, 3654; c) P. C. Hariharan, J. A. Pople, *Theor. Chim. Acta* **1973**, *28*, 213.
[52] a) A. D. Becke, *J. Chem. Phys.* **1993**, *98*, 5648; b) C. Lee, W. Yang, R. G. Parr, *Phys. Rev. B* **1988**, *37*, 785.
[53] B. J. Lynch, P. L. Fast, M. Harris, D. G. Truhlar, *J. Phys. Chem. A* **2000**, *104*, 7650.
[54] Jaguar 6.0 treats solvated molecular systems with the SCRF method, using its own Poisson–Boltzmann solver, which makes it possible to compute solvation energies and minimum-energy solvated structures of solvated transition states. For details see: a) D. J. Tannor, B. Marten, R. Murphy, R. A. Friesner, D. Sitkoff, A. Nicholls, M. Ringnalda, W. A. Goddard III, B. Honig, *J. Am. Chem. Soc.* **1994**, *116*, 11875; b) B. Marten, K. Kim, C. Cortis, R. A. Friesner, R. B. Murphy, M. N. Ringnalda, D. Sitkoff, B. Honig, *J. Phys. Chem.* **1996**, *100*, 11775; c) C. J. Cramer, D. G. Truhlar, *Chem. Rev.* **1999**, *99*, 2161.

Received: January 30, 2009
Published Online: April 6, 2009

